International Journal of Heat and Mass Transfer 55 (2012) 7104–7108

Contents lists available at SciVerse ScienceDirect

International Journal of Heat and Mass Transfer

journal homepage: www.elsevier.com/locate/ijhmt

Fluidic lens by using thermal lens effect

Hong Duc Doan *, Yoshihiko Akamine, Kazuyoshi Fushinobu

Department of Mechanical and Control Engineering, Tokyo Institute of Technology, Box I6-3, Meguro-ku, Tokyo 152-8550, Japan

ARTICLE INFO

Article history:
Received 18 April 2012
Received in revised form 6 July 2012
Accepted 10 July 2012
Available online 3 August 2012

Keywords:
Fluidic lens
Thermal lens effect
Pump power
Pump intensity profile

ABSTRACT

This research presents a novel fluidic lens based on thermal lens effect. Effects of the pump power and the pump beam intensity distribution to the probe beam profile in the dual thermal lens system are investigated experimentally and theoretically. A model, which accounts for heat conduction, natural heat convection and ray tracing in inhomogeneous medium is developed to predict the characteristics of the thermal lens system. Numerical results show the advantage of the uniform pump beam in reducing the spherical aberration compared with the Gaussian pump beam. An experiment with the uniform pump beam is carried out to confirm the numerical prediction. Experimental results show a good agreement with the calculated results. Finally, the pump power is varied to adjust the focal length of the system.

1. Introduction

Recently the development of the fluidic optical devices has attracted great attention due to various advantages of these devices, including flexibility of optical parameters, versatility and reconfigurability [1]. Several novel fluidic optical devices, for example, a liquid-core, liquid-cladding waveguide consist of two streams of liquids with lower refractive index, sandwiching a stream of liquid with higher refractive index flowing in a microchannel [2–4]; the fluidic diffraction grating using immiscible fluids [5–6]; miniature optical sensing [7]; fluidic tunable micro lens and micro lens array [8–11], have been demonstrated.

Of many optical components, fluidic lenses are well known to present significant advantages for wide range of applications from mobile phone to lab-on-a-chip. Compared with traditional lenses, fluidic lenses have a number of apparent advantages such as tunable refractive index and reconfigurable geometry. Several approaches to design the fluidic lens have been developed based on the microfluidic techniques to modify the liquid lens shape by using: out-of-plane micro-optofluidic [12–13], in-plane micro-optofluidic [14–15], electron wetting [16], dielectrophoresis [17], hydrodynamic force [18]. Other approaches are based on tuning the refractive index of the liquid by other means such as pressure control, optical control, magnetic control, thermo-optic control, and electro-optic control.

In this research, a concept of a tunable divergence lens for collimator in laser processing based on gradient refractive index of liquid (GRIN-L). GRIN-L lens is established by controlling the temperature field generated in thermal lens effect. A schematic of the concept is shown in Fig. 1. By controlling the temperature field as well as refractive index distribution of liquid medium, the refractive angle of each light ray passing through the liquid medium can be controlled to focal all of the light ray to the focal point. Authors have examined the effect of the one dimensional temperature profile perpendicular to the incident beam direction and the resulting natural convection on the beam bending [19]. A 2D model in cylindrical coordinate that incorporates the natural convection effect is used to well predict the intensity distribution of the probe beam after passing through liquid medium [20]. This model is applied to develop a fluidic laser beam shaper [20]. In this research, the intensity profile and the power of the pump beam are changed to evaluate the quality and optical parameter of the GRIN-L lens both experimentally and theoretically.

2. Principle of fluidic lens

When the liquid medium is irradiated by laser light, local heating near the beam axis produces a radially dependent temperature distribution.The distribution creates the distribution of the refractive index of the liquid medium, and in particular, lower refractive index in the region near the beam center is observed. As a consequence, the radius of curvature of the wave front at the region near the beam center is shorter than the one at the wing. The liquid medium behaves as a convergence GRIN-L lens with focal length depending on the radial position of the incident ray relative to the optical axis of the cuvette. The ray equation that is solved numerically to obtain the path of an incident beam is given as:

$$\frac{d}{ds}\left(n\frac{dR}{ds}\right) = \mathrm{grad}(n) \tag{1}$$

* Corresponding author. Tel.: +81 03 5734 2500; fax: +81 03 5734 2500.
E-mail address: doan.d.aa@m.titech.ac.jp (H.D. Doan).

0017-9310/$ - see front matter © 2012 Elsevier Ltd. All rights reserved.
http://dx.doi.org/10.1016/j.ijheatmasstransfer.2012.07.024

Nomenclature

a	thermal diffusivity, m^2/s
c	concentration, mol/L
d	distance from the cuvette to the detector of the CCD camera, m
g	acceleration of gravity, m/s^2
L	sample thickness, m
n	refractive index of liquid medium
n_0	refractive index of liquid medium at 20°C
R	differential element of the path length
p	pressure, Pa
P	power of laser, W
S	heat source, K/s
T	temperature, K
r, z	coordinate, m
v_r, v_z	velocity in r, z direction, m/s
r_0	beam radius, m

Greek symbols

α	absorption coefficient, cm^{-1}
β	coefficient of volume expansion,K^{-1}
λ	laser beam wavelength, nm
ρ	density of liquid medium, kg/m^3
Φ	beam waist (FWHM), m
θ	divergence of the laser beam, mrad
ν	kinematic viscosity, m^2/s

Here, ds and R are the differential element of the path length and the positional vector of the ray, respectively. The variable n is the refractive index of the liquid sample and is a function of the temperature distribution as:

$$n(T) = n_0 + \frac{dn}{dT}(T - T_0) \tag{2}$$

Here, $n_0 = 1.359$ is the refractive index of the liquid medium at reference temperature, $T_0 = 298.15$ K, and dn/dT is the temperature coefficient of the refractive index. In this study, it is considered that the change of refractive index is caused only by the temperature change of the liquid medium and the thermal coefficient of the refractive index, dn/dT, and the concentration are assumed to be constant over the range of the temperature rise induced by the pump beam. The temperature distribution in the liquid medium in steady state is calculated numerically by solving the following governing equations:

$$\frac{1}{r}\frac{\partial}{\partial r}(r v_r) + v_z\frac{\partial v_z}{\partial z} = 0 \tag{3}$$

$$v_r\frac{\partial v_r}{\partial r} + v_z\frac{\partial v_r}{\partial z} = -\frac{1}{\rho}\frac{\partial p}{\partial r} + \nu\left(\frac{\partial}{\partial r}\left(\frac{1}{r}\frac{\partial}{\partial r}(r v_r)\right) + \frac{\partial^2 v_r}{\partial z^2}\right) \tag{4a}$$

$$v_r\frac{\partial v_z}{\partial r} + v_z\frac{\partial v_z}{\partial z} = -\frac{1}{\rho}\frac{\partial p}{\partial z} + \nu\left(\frac{1}{r}\frac{\partial}{\partial r}\left(r\frac{\partial v_z}{\partial r}\right) + \frac{\partial^2 v_z}{\partial z^2}\right) + g\beta(T - T_0) \tag{4b}$$

$$v_r\frac{\partial T}{\partial r} + v_z\frac{\partial T}{\partial z} = a\left(\frac{1}{r}\frac{\partial}{\partial r}\left(r\frac{\partial T}{\partial r}\right) + \frac{\partial^2 T}{\partial z^2}\right) + S \tag{5}$$

$$S = \frac{\alpha e^{-\alpha z} I_0(r)}{\rho C_p} \tag{6}$$

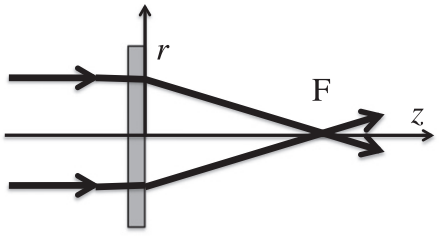

Fig. 1. Concept of fluidic lens by using thermal lens effect.

Here, $I_0(r)$ is intensity distribution of the pump laser, and the spot size of the laser beam is assumed to be constant through the interaction volume within the liquid medium. The temperature distribution is calculated numerically by using the finite difference method. The 1st order upwind scheme and a center the 2nd order are applied to discretize the advection term and the diffusion term, respectively. The thermophysical properties of the liquid medium can be found in Ref. [20].

3. Influence of the pump beam profile

Influence of the pump beam profile to the focal length of the GRIN-L lens was investigated numerically with the calculation conditions in Table. 1. The intensity profile of the pump beam is applied either with the Gaussian distribution or the quasi-flat-top distribution (a super-Gaussian distribution of order k) as shown in Eq. (7) or Eq. (8).

$$I_{\text{Gaussian}} = \frac{2P}{\pi r_0^2}\exp\left(\frac{-2r^2}{r_0^2}\right) \tag{7}$$

$$I_{\text{Flat-top}} = \frac{Pk2^{2/k}}{2\pi r_0^2\Gamma(2/k)}\exp\left(\frac{-2r^k}{r_0^k}\right) \tag{8}$$

Here, Γ is the Gamma function. Variables r, r_0 and P are the distance from the laser axis, the beam radius and the power of the pump laser, respectively. In this calculation, quasi-flat-top beam is the 10 order of the super-Gaussian distribution. Two types of the pump intensity profile are shown in Fig. 2.

The effect of the pump beam profile to the focal length of the GRIN-L lens is shown in Fig. 3. The vertical and horizontal axes show the focal length and the distance from laser axis, respectively. The solid and dashed lines represent the plot of the focal length to the radial position of the incident ray relative to the optical axis of the cuvette in the case of the Gaussian pump beam and the quasi flat-top pump beam, respectively. As shown in Fig. 3, for the Gaussian pump beam the absolute value of the focal length of the GRIN-L lens increases sharply with increasing of the distance from laser axis, which means larger spherical aberration. In this case, the center of the probe beam, which passing through shorter focal length,

Table 1
Calculation conditions.

Pump power, mW	10
Pump beam diameter, mm	1.5
Absorption coefficient, cm^{-1}	2.0

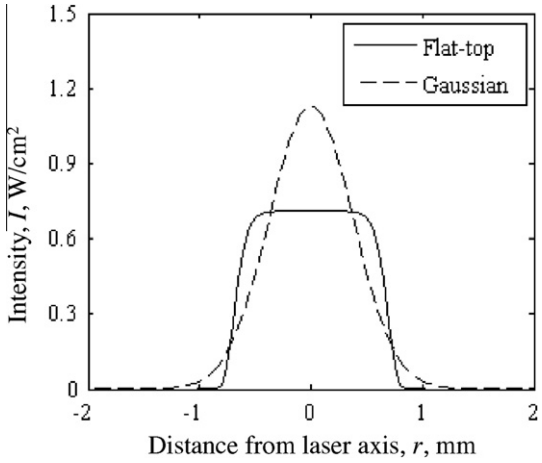

Fig. 2. Two types of the pump beam profile. The vertical and horizontal axes show the intensity and the distance from laser axis, respectively.

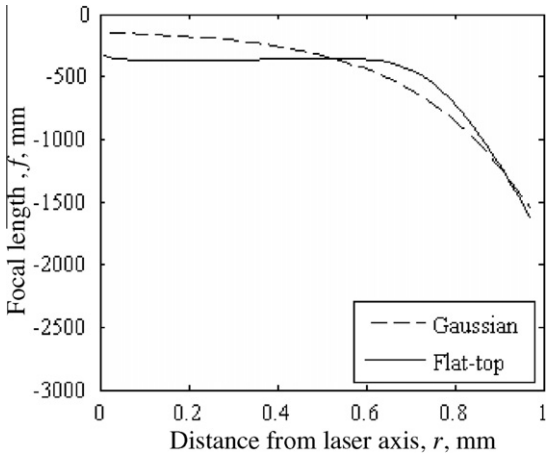

Fig. 3. Effect of the pump beam profile to the focal length of the GRIN-L lens. The vertical and horizontal axes show the focal length and the distance from laser axis, respectively.

spreads out more rapidly than the beam wing. As a consequence, the further the propagation distance of the probe beam, the laser beam profile changes from Gaussian to the doughnut beam profile [20], which should cause some undesirable results in laser processing [21]. In contrast, with the quasi flat-top pump beam, the focal length of the GRIN-L lens varies lightly with the increase of the distance from laser axis within the beam waist of the flat-top pump beam. The area within the beam waist of the quasi flat-top pump beam acts as a divergent lens with small spherical aberration. Therefore, the uniform pump beam shows the advantage of reducing the spherical aberration for the purpose of designing the GRIN-L lens.

4. Experimental set-up

In order to confirm the qualities of the GRIN-L lens, an experiment with the quasi flat-top pump beam is carried out as shown in Fig. 4.A CW diode blue laser is used as the pump laser (P = 10 mW, λ = 488 nm, Φ = 0.69 mm, TEM_{00}). A cuvette has a three-layer structure with a sheet copper sandwiched between 2 pieces of fused silica. The height of the fused silica is 1 mm. The sheet copper has doughnut shape. The liquid sample contained inside the doughnut hole has the same height with the sheet copper.

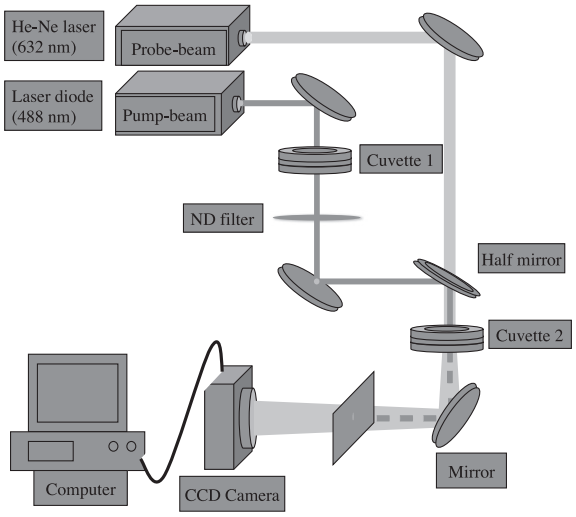

Fig. 4. Experimental set up for the fluidic divergent lens with a dual-beam thermal lens system.

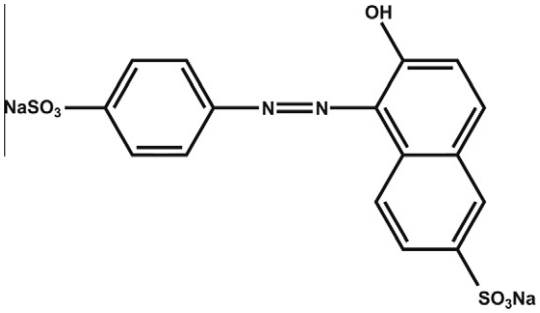

Fig. 5. Molecular formula of the Sunset-yellow.

By varying the height of the sheet copper, the height of the liquid medium can be changed. The ethanol solution with a dye, Sunset-yellow, dissolved is filled in the cuvette. The chemical formula of the Sunset-yellow is shown in Fig. 5. In "cuvette 1", the height of the liquid medium is 0.5 mm, and the absorption coefficient is 2.92 cm^{-1} (at wavelength of 488 nm). In "cuvette 2", the thickness of liquid is 1 mm, and the absorption coefficient is 55 cm^{-1} (at wavelength of 488 nm). A CW He-Ne laser is used as the probe laser (P = 0.6 mW, λ = 632 nm, Φ = 0.8 mm, TEM_{00}). It is noted that the light absorption in ethanol solution can be ignored at the wavelength of the probe laser. First, the pump beam passes through cuvette1. The beam profile of the pump beam was converted from the Gaussian beam to the flat-top beam during its transmission through cuvette 2 as shown in Fig. 6.Then, the probe beam was adjusted to overlap with the pump beam. After propagating through the sample, the probe beam light is directed toward the CCD camera, and the pump beam is blocked using a filter located at the detection plane. The distance between cuvette 2 and CCD camera is varied, and the $1/e^2$ diameter of probe beam is measured.

Fig. 7 shows the change along the propagation direction in the profile of the probe beam. The vertical and horizontal axes show the intensity and the distance from the laser axis, respectively. By using the quasi flat-top pump beam, the beam profile of probe laser can remain in Gaussian distribution during its propagation. Fig. 8 shows the plot of the beam waist of the probe beam again its propagation distance from cuvette 2 to CCD camera. As shown in Fig. 8, the waist of the probe beam varies linearly with its propagation distance. In other words, cuvette 2 acts as a divergence lens

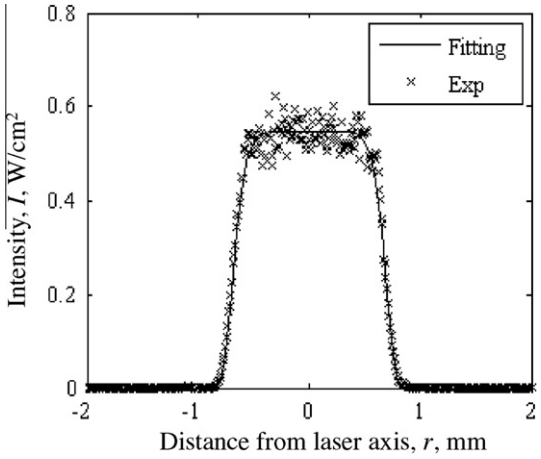

Fig. 6. The intensity profile of the pump beam during its transmission through cuvette 2. Dotted and solid lines show the measured result by using the CCD camera and their fitting by super-Gaussian distribution, respectively.

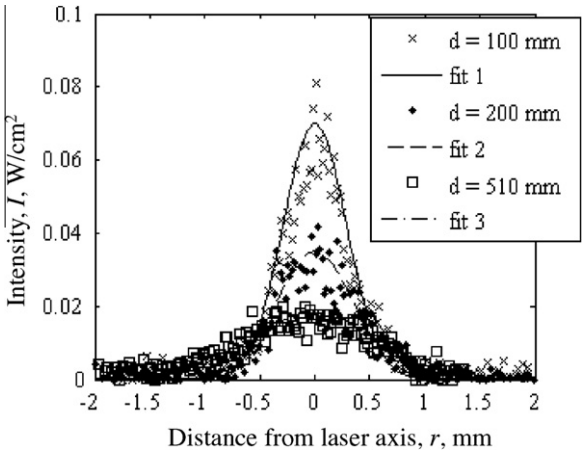

Fig. 7. The change along the propagation direction in the profile of the probe beam. The vertical and horizontal axes show the intensity and the distance from the laser axis, respectively.

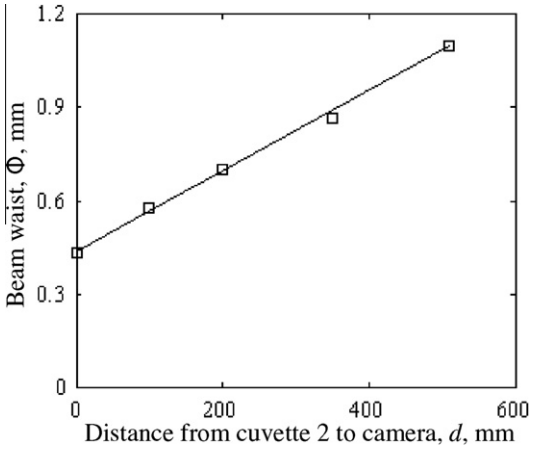

Fig. 8. The change along the propagation direction in the waist (the $1/e^2$radius) of the probe beam.The vertical and horizontal axes show the beam waist and the distance from cuvette 2 to CCD camera, respectively.

with focal length of $f = -424$ mm, which is calculated by considering the divergence angle of probe laser $\theta = 1.2$ mrad.

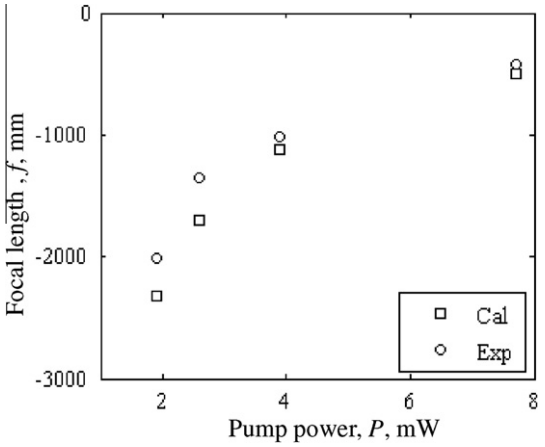

Fig. 9. Relationship between the pump power and the focal length. The horizontal and vertical axes show the pump power and focal length, respectively. The pump power is changed from 1 to 8 mW.

Next, the pump power is changed from $P = 7.7$ mW to $P/2$, $P/3$ and $P/4$, respectively. The distance from cuvette 2 to CCD camera is fixed at 510 mm, and the waist of the probe beam is measured. Fig. 9 shows the plots of beam waist against the pump power. The horizontal and vertical axes show the pump power and the focal length, respectively. Square and circle dots show calculated and experimental results, respectively. Calculated results are the average value of the focal length during the distance smaller than the waist of the flat-top pump beam from laser axis. Both calculated and experimental results show that focal length of GRIN-L lens increase with the increase of the pump power. As shown in Fig. 9, calculated and experimental results show good agreement, especially at high power region of the pump beam, and increasing discrepancies at lower pump power. To explain in detail of the discrepancy in low pump power regime, the focal length depends on the radial position of the incident ray was calculated and shown in Fig. 10. As mentioned in the previous works of Tidwell et al. [22] and MacDonald et al. [23], if the heat flow is purely radial and the pump beam has a perfect flat-top profile, the temperature profile becomes parabolic and the cuvette acts like a divergent lens. However, in the practical situation, because of the cooling effect of the glass window in cuvette, the parabolic temperature profile in radial direction is perturbed in temperature field near the glass window.

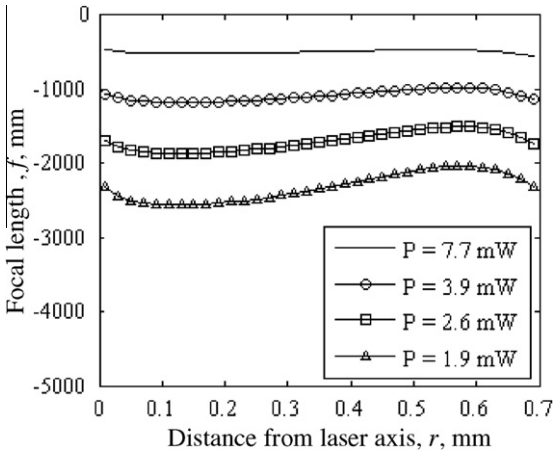

Fig. 10. Focal length depends on the radial position of the incident ray at difference pump power. The vertical and horizontal axes show focal length and distance from laser axis, respectively.

As a consequence, the perturbation of the temperature profile causes the spherical aberration. When the power of the pump beam is large, the perturbation is small compared with the lens effect as shown in Fig. 10 and the model of the average value of the focal length show a good agreement with experimental results. However, with the decrease of the pump power, the perturbation becomes large compared with the lens effect, and the ideal parabolic model is no longer valid and the spherical aberration increases.This means that, by adjusting the pump power, the focal length can be controlled, while keeping spherical aberration relatively smaller.

5. Conclusions

In this research, a novel idea of fluidic divergent lens is demonstrated. The fluidic lens is based on controlling some parameters in the thermal lens system. The interactions among the intensity profile of the pump beam, the pump power and the spherical aberration have been investigated experimentally and theoretically. It is demonstrated that the uniform pump beam shows the advantage of reducing the spherical aberration for the purpose of designing the GRIN-L lens. The focal length can be controlled easily by adjusting the pump power while the lower pump power causes the large spherical aberration. With some merits as flexible, versatile and low cost, this method will be a promising tool in many fields of laser applications.

Acknowledgement

Part of this work has been supported by the Grant-in-Aid for JSPS Fellows and Grant-in-Aid for Scientific Research of MEXT/JSPS.

References

[1] G.M. Whitesides, S.K.Y. Tang, Fluidic optics, Proc. SPIE 6329 (2006) 63290A.
[2] D.B. Wolfe, R.S. Conroy, P. Garstecki, B.T. Mayers, M.A. Fischbach, K.E. Paul, M. Prentiss, G.M. Whitesides, Dynamic control of liquid-core, liquid-cladding optical waveguides, Proc. Natl. Acad. Sci. USA 101 (2004) 12434.
[3] R.S. Conroy, B.T. Mayers, D.V. Vezenov, D.B. Wolfe, M.G. Prentiss, G.M. Whitesides, Optical waveguiding in suspensions of dielectric particles, Appl. Phys. Lett. 44 (2005) 7853.
[4] S.K.Y. Tang, B.T. Mayers, D.V. Vezenov, G.M. Whitesides, Optical waveguiding using thermal gradients across homogeneous liquids in microfluidic channels, Appl. Phys. Lett. 88 (2006). 061112/1.
[5] P. Garstecki, I. Gitlin, W. DiLuzio, G.M. Whitesides, Formation of monodisperse bubbles in a microfluidic flow-focusing device, Appl. Phys. Lett. 85 (2004) 2649.
[6] P. Garstecki, M.J. Fuerstman, H.A. Stone, M. Whitesides George, Formation of droplets and bubbles in a microfluidic T-junction - scaling and mechanism of break-up, Lab Chip 6 (2006) 437.
[7] L. Saurei, G. Mathieu, B. Berge, Design of an autofocus lens for VGA 1/4 - in CCD and CMOS sensors, Proc. SPIE: Inter. Soc. Opt. Eng. 5249 (2004) 288.
[8] M. Agarwall, R.A. Gunasekaran, P. Coane, K. Varahramyan, Polymer-based variable focal length microlens system, J. Micromech. Microeng. 14 (2004) 1665–1673.
[9] J. Chen, W.S. Wang, J. Fang, K. Varahramyan, Variable-focusing microlens with microfluidic chip, J. Micromech. Microeng. 14 (2004) 675–680.
[10] J. Aizenberg, G. Hendler, Designing efficient microlens arrays: lessons from Nature, J. Mater. Chem. 14 (2004) 2066.
[11] N. Chronis, G.L. Liu, K.H. Jeong, L.P. Lee, Tunable liquid-filled microlens array integrated with microfluidic network, Opt. Exp. 11 (2003) 2370–2378.
[12] S.H. Ahn, Y.K. Kim, Proposal of human eye's crystalline lens-like variable focusing lens, Sens. Actuators, A 78 (1999) 48.
[13] D.Y. Zhang, V. Lien, Y. Berdichevsky, J.H. Choi, Y.H. Lo, Fluidic adaptive lens with high focal length tenability, Appl. Phys. Lett. 82 (2003) 3171.
[14] S.K. Hsiung, C.H. Lee, G.B. Lee, Microcapillary electrophoresis chips utilizing controllable micro-lens structures and buried optical fibers for on-line optical detection, Electrophoresis 29 (2008) 1866.
[15] V. Lien, Y. Berdichevsky, Y.H. Lo, Microspherical surfaces with predefined focal lengths fabricated using microfluidic capillaries, Appl. Phys. Lett. 83 (2003) 5563.
[16] C.B. Gorman, H.A. Biebuyck, G.M. Whitesides, Control of the shape of liquid lenses on a modified gold surface using an applied electrical potential across a self-assembled monolayer, Langmuir 11 (1995) 2242.
[17] C.C. Cheng, C.A. Chang, H.A. Yeh, Variable focus dielectric liquid droplet lens, Opt. Exp. 14 (2006) 4101.
[18] S.K.Y. Tang, C.A. Stan, G.M. Whitesides, Dynamically reconfigurable liquid-core liquid-cladding lens in a microfluidic channel, Lab Chip 8 (2008) 395.
[19] H.D. Doan, K. Fushinobu, K. Okazaki, Investigation on the interaction among light, material and temperature field in the transient lens effect, transmission characteristics in 1D temperature field, Proc. ITherm 2010 (2010) 127.
[20] H.D. Doan, Y. Akamine, K. Fushinobu, Fluidic laser beam shaper by using thermal lens effect, Int. J. Heat Mass Transfer 55 (2012) 2807–2812.
[21] D.H. Doan, Y. Yin, N. Iwatani, K. Fushinobu, Laser processing by using fluidic laser beam shaper, in: Proc. National Heat Transfer Symposium, 2012, pp. 547–548.
[22] S.C. Tidwell, J.F. Seamans, M.S. Bowers, A.K. Cousins, Scaling CW diode-end-pumped Nd:YAG lasers to high aver- age powers, IEEE J. Quant. Electron. 28 (4) (1992) 997–1009.
[23] M.P. MacDonald, Th. Graf, J.E. Balmer, H.P. Weber, Reducing thermal lensing in diode-pumped laser rods, Opt. Commun. 178 (2000) 383–393.